

## Supporting information

### **Pt(II) as an active site supported on superhydrophilic nickel foam with boosted electrocatalytic hydrogen evolution performance**

Yi Wei,<sup>a,b,s</sup> Caleb Gyan-Barimah,<sup>a,s</sup> Ling Li,<sup>b,s</sup> Jong Hun Sung,<sup>a</sup> Muhammad Irfansyah Maulana,<sup>a</sup> Ha-Young Lee,<sup>a</sup> Chao Han,<sup>\*b</sup> and Jong-Sung Yu<sup>\*a</sup>

<sup>a</sup> Department of Energy Science and Engineering, Daegu Gyeongbuk Institute of Science and Technology (DGIST), Daegu 42988, Republic of Korea

<sup>b</sup> School of Materials Science and Engineering, Central South University, Changsha 410083, China

## EXPERIMENTAL SECTION

**Preparation of NiF(H).** To prepare NiF(H), a piece of NF (size: 0.5 cm × 0.5 cm) was immersed into 1.0 M hydrochloric acid (HCl) under ultrasonication treatment for 3 min, followed by washing with water several times. For the hydrophobic NiF, the HCl was replaced with ethanol and acetone. The washed NiF and NiF(H) were collected and then dried at 60 °C for 6h.

**Preparation of catalysts.** The binder-free Pt(II)/NiF(H) sample was prepared by a simple wetting method. Firstly, 10 μL H<sub>2</sub>PtCl<sub>6</sub> solution (100 mg<sub>Pt</sub>/mL) was added into mixed solution (mixed 5 mL water and 5 mL ethanol solution ( $V_{\text{water}}: V_{\text{ethanol}} = 1:1$ )) and stirred until the homogeneous solution was formed. Then, the NiF(H) (size: 5mm × 5mm) was immersed in the above solution quickly taken out from the solution, and then treated in an electric oven at 25 °C for 12 h before electrochemical testing. The as-prepared sample was labeled as Pt(II)/NiF(H). For comparison, the Pt(II)/NiF was also prepared by using the same experimental condition except that NiF was used instead of NiF(H). Pt(0) coated on NiF (Pt(0)/NiF) and NiF(H) (Pt(0)/NF(H)) are also prepared. The Pt(0)/NiF is prepared by reducing the Pt(II)/NiF(H) under H<sub>2</sub>/Ar (5%/95%) atmosphere at 300 °C for 1 h. The Pt(0)/NiF is treated in 1.0 M HCl for 1 min, and then washed with water 5 times to obtain Pt(0)/NiF(H). The Pt loading amount is determined by the inductively coupled plasma-optical emission spectrometry (ICP-OES) for each catalyst. For comparison of catalytic performance. PtC(20 wt%)/NiF is prepared. Pt/C(20 wt%) catalyst (5 mg) and 250 μL Nafion (5%) solution were added into 9.75 mL mixed water and ethanol solution ( $V_{\text{water}}: V_{\text{ethanol}} = 1:1$ ). Then, the PtC was loaded on NiF with a Pt mass loading of 0.1 mg cm<sup>-2</sup>.

**Characterization.** Powder X-ray diffraction (XRD) data was recorded using a Rigaku Smartlab diffractometer with Cu-Kα (0.15406 nm) operated at 40 kV and 40 mA at a scan rate of 4° min<sup>-1</sup>. X-ray photoelectron spectroscopy (XPS) analyses were operated with an AXIS-NOVA (Kratos) X-ray photoelectron spectrometer using a monochromated Al Kα X-ray source (hν = 1486.6 eV) operated at 150 W under a base pressure of 2.6 × 10<sup>-9</sup> Torr. Binding energies were calibrated by setting C 1s peak to 284.6 eV. The XPS spectra were deconvoluted using the curve fitting program, CasaXPS. The scanning electron microscopy (SEM) images were obtained using a Hitachi S-4700 microscope operated at an acceleration voltage of 10 kV. The transmission electron microscope (TEM), high-resolution transmission electron microscope (HR-TEM), and scanning TEM (STEM), as well as EDS spectra and elemental mapping, were obtained using a Themis Z. The water droplet (drop volume of 5 μL) was used as an indicator in the experiment to characterize the wetting property of the samples. A water contact angle was obtained by Drop Shape Analyzer (DSA100). The digital photographs of water droplets on

surfaces were obtained by a digital camera (Sony). X-ray absorption near edge structure (XANES) and extended X-ray absorption fine structure (EXAFS) at the Ni, Cu K-edge were conducted at the synchrotron center Pohang Accelerator Laboratory with beamline number 8 C. All the XAS data were recorded at room temperature using the Transmittance mode. The XANES and EXAFS spectra were fitted using the Athena and Artemis software packages. Raman scattering was performed on the LabRAM HR800 system under an excitation of 532 nm laser. The potential was controlled by a potentiostat (Biologic SP150e). The spectra were collected using 30 s exposure and accumulated in duplicate at different potentials.

### **Electrochemical measurements.**

The electrochemical characterizations were carried out with a potentiostat (Biologic VMP3) at room temperature in 1.0 M KOH electrolyte using a three-electrode configuration that contains Pt wire as the counter electrode, an Ag/AgCl (saturated KCl) as the reference electrode and the prepared NiF based catalysts as the working electrode. The cyclic voltammetry (CV) curves were recorded with a scan rate of 50 mV s<sup>-1</sup>. The LSV polarization curves were conducted at a rate of 1 mV s<sup>-1</sup> in an Ar-saturated 1.0 M KOH solution after 10 CV cycles. The electrochemical impedance spectroscopy (EIS) measurements were carried out in the frequency range of 100 kHz to 0.1 Hz. The chronopotentiometry was carried out under a constant current density of 10 mA cm<sup>-2</sup> in an Ar-saturated 1.0 M KOH solution. Double-layer capacitance ( $C_{dl}$ ) was calculated by performing CV measurements at different scan rates of 20, 40, 60, 80, and 100 mV s<sup>-1</sup> in the potential range of 0.05-0.17 V (vs RHE) for NiF and NiF(H), 0.4-0.5 V (vs RHE) for Pt(II)/NiF and Pt(II)/NiF(H). The value of  $C_{dl}$  was obtained from plotting  $\Delta j = j_a - j_c$  at 0.11 V for NiF and NiF(H), 0.45 V for Pt(II)/NiF and Pt(II)/NiF(H) against the scan rates ( $j_a$  and  $j_c$  are anode and cathode current density, respectively). All electrode potentials were calibrated into the reversible hydrogen electrode (RHE) according to the Nernst equation:  $E_{RHE} = E_{Ag|AgCl} + 0.197 \text{ V} + 0.059 \times \text{pH}$ . The iR drop was compensated at 70 % through the positive feedback model.

### **Density functional theory calculations.**

All the DFT calculations were conducted based on the Vienna Ab initio Simulation Package (VASP)<sup>[1-2]</sup>. The exchange-correlation potential was described by the Perdew–Burke–Ernzerhof (PBE) generalized gradient approach (GGA)<sup>[3]</sup>. The electron-ion interactions were accounted for by the projector augmented wave (PAW)<sup>[4]</sup>. All DFT calculations were performed with a cut-off energy of 400 eV, and the Brillouin zone was sampled using the 2 × 2 × 1 K-point. The energy and force convergence criteria of the self-consistent iteration were set to 10<sup>-5</sup> eV and 0.02 eV Å<sup>-1</sup>, respectively. Besides, the DFT + U

correction for Ni, and Pt atoms was considered, and the U-J value of 5.5 for Ni, and 3.0 eV for Pt. The DFT-D3 method was used to describe van der Waals (vdW) interactions [5]. VESTA software was used to visualize the results [6].

The Gibbs free energy changes ( $\Delta G$ ) of the reaction are calculated using the following formula:

$$\Delta G = \Delta E + \Delta ZPE - T\Delta S + \Delta G_U + \Delta G_{\text{pH}}$$

Where  $\Delta E$  is the difference of electron energies calculated by DFT;  $\Delta ZPE$  and  $\Delta S$  are the changes of zero-point energy and entropy, respectively, which are obtained from vibrational frequencies.  $T$  is the temperature (298.15 K).  $\Delta G_U = -eU$ , where  $U$  is the applied electrode potential.  $\Delta G_{\text{pH}} = k_B T \times \ln 10 \times \text{pH}$ , where  $k_B$  is the Boltzmann constant.

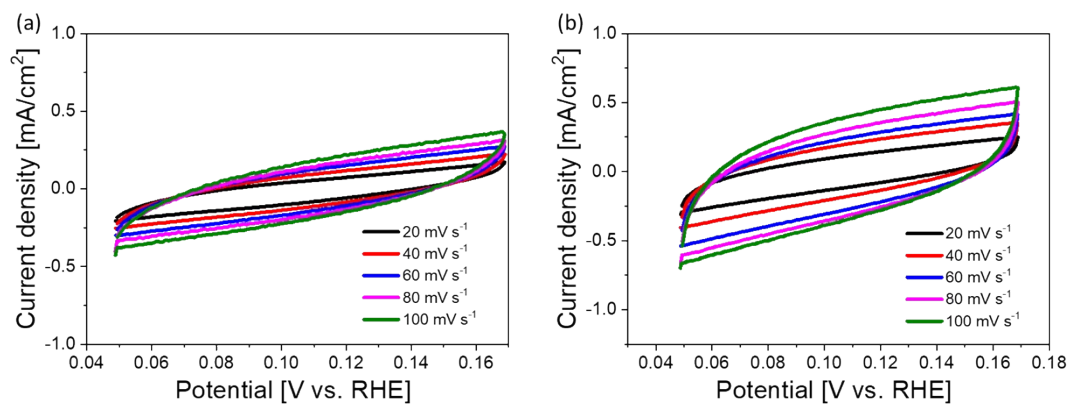


**Figure S1.** CV curves of (a) NiF and (b) NiF(H) from 0.05 V to 0.17 V vs RHE at different scan rates.

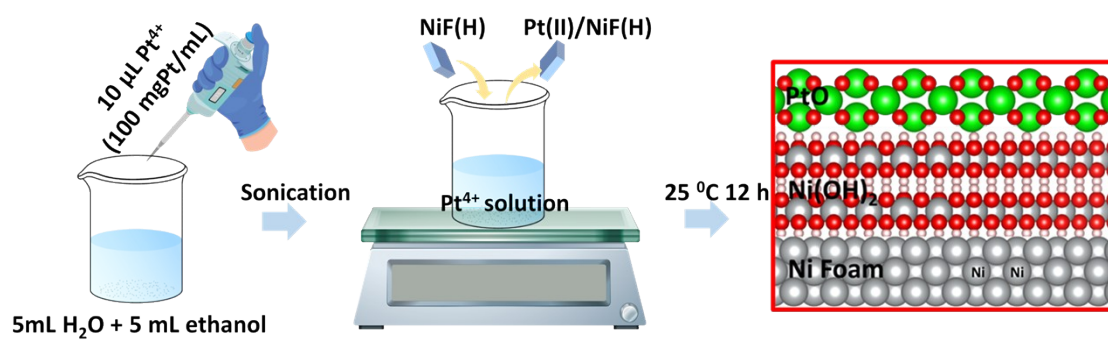


**Figure S2.** The preparation process of Pt(II)/NF(H) by a simple fast dip-coating method.

**Table S1.** Pt loading on NiF and NiF(H) as determined from ICP-OES.

Sample	Pt(II)/NiF(H)	Pt(II)/NiF	Pt(0)/NiF(H)	Pt(0)/NiF
Pt loading	11.7	12.2	10.9	11.4
ammount	( $\mu\text{g cm}^{-2}$ )			

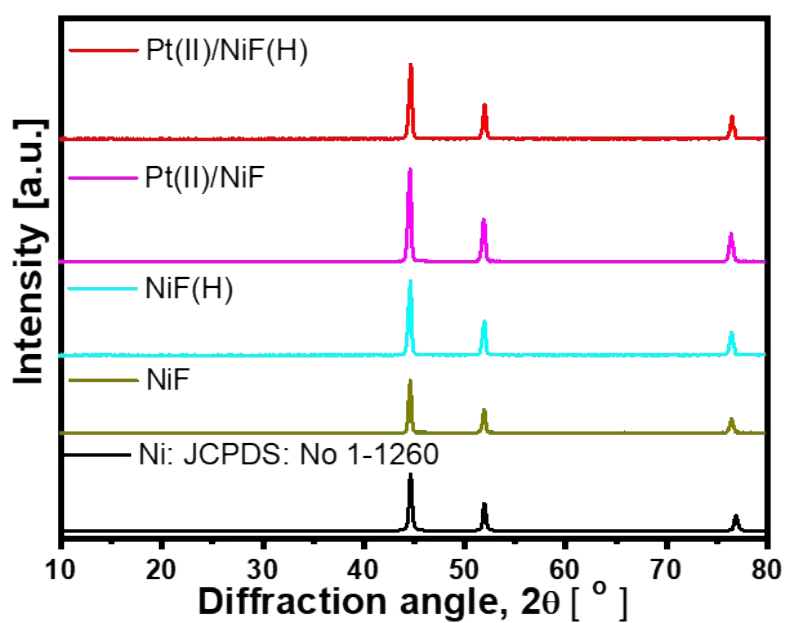


**Figure S3.** XRD patterns of NiF, NiF(H), Pt(II)/NiF, and Pt(II)/NiF(H).

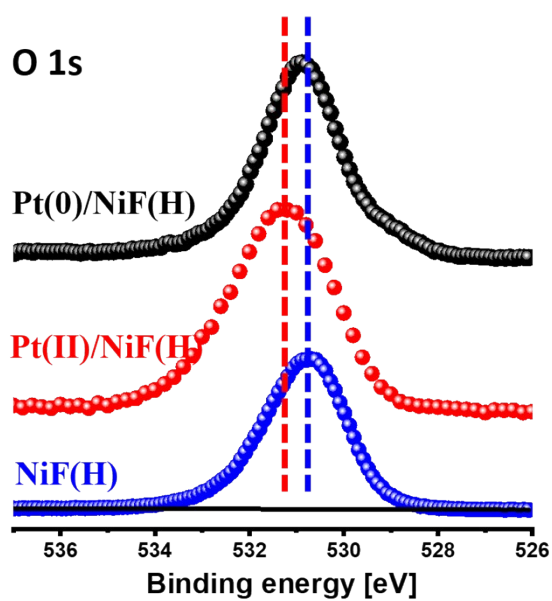


**Figure S4.** O 1s XPS spectra of Pt(II)/NiF, Pt(II)/NiF(H) and Pt(0)/NiF(H).

**Table S2.** Pt loading amount on NiF(H) at different solution concentrations as determined from ICP-OES.

Sample	5 $\mu\text{L}$	10 $\mu\text{L}$	20 $\mu\text{L}$
Pt loading	5.2	11.7	24.5
ammount	( $\mu\text{g cm}^{-2}$ )	( $\mu\text{g cm}^{-2}$ )	( $\mu\text{g cm}^{-2}$ )

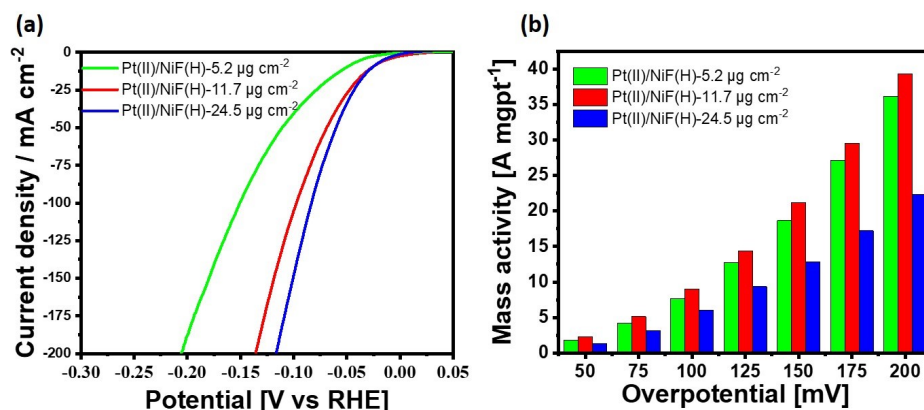


**Figure S5.** (a) LSV curves and (b) histogram of mass activities of Pt(II)/NiF(H) at different Pt mass loading.

The overpotentials of Pt(II)/NiF(H)-5.2  $\mu\text{g cm}^{-2}$ , Pt(II)/NiF(H)-11.7  $\mu\text{g cm}^{-2}$ , and Pt(II)/NiF(H)-24.5  $\mu\text{g cm}^{-2}$  are 50.6, 26.4 and 26.1 mV, at -10  $\text{mA cm}^{-2}$  respectively, indicating an increase in performance with Pt loading amount. Interestingly, there is only a minute difference in overpotential between Pt(II)/NiF(H)-11.7  $\mu\text{g cm}^{-2}$  and Pt(II)/NiF(H)-24.5  $\mu\text{g cm}^{-2}$  in the low current density regions, indicating the electrocatalytic performance is not significantly influenced above a certain Pt loading threshold (here 11.7  $\mu\text{g cm}^{-2}$ ). This is evidenced in the LSVs illustrated in Figure S5a, where Pt(II)/NiF(H)-11.7  $\mu\text{g cm}^{-2}$  exhibits the best mass activity amongst the other control samples (Figure S5b). Therefore, the optimized Pt mass loading in Pt(II)/NiF(H) is 11.7  $\mu\text{g cm}^{-2}$ .

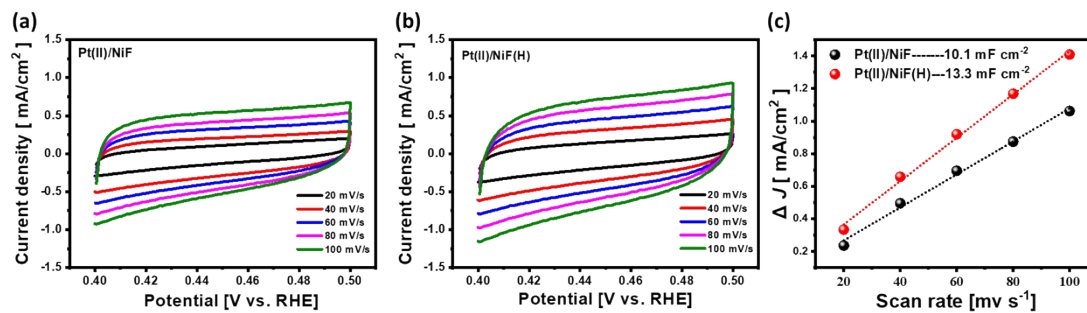


**Figure S6.** ECSA analysis by CV method. CVs of (a) Pt(II)/NiF and (b) Pt(II)/NiF(H), (c) Plots showing the dependence of current density on the scan rate for the extraction of double-layer capacitance ( $C_{dl}$ ) performed on Pt(II)/NiF and Pt(II)/NiF(H).

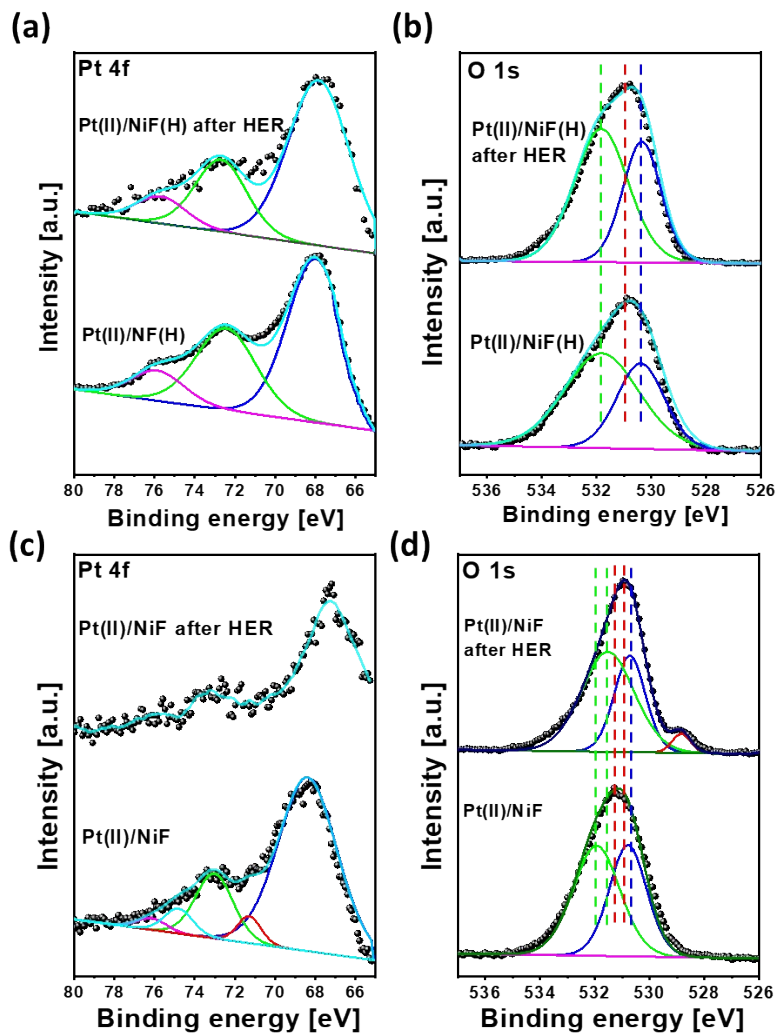


**Figure. S7.** XPS spectra showing (a) Pt 4f and (b) O 1s from Pt(II)/NiF(H). High-resolution (c) Pt 4f and (d) O 1s from Pt(II)/NiF before and after long-term durability test in Figure 4d.

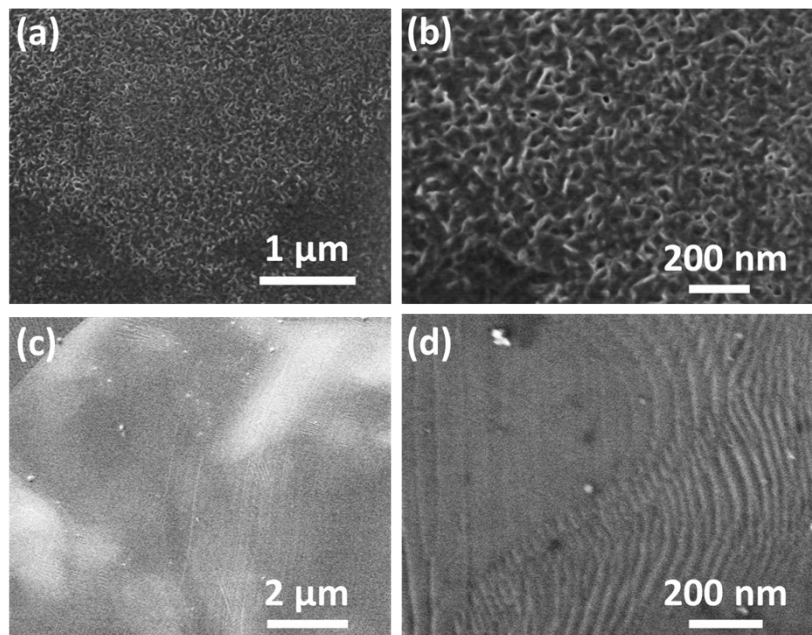


**Figure S8.** SEM images of (a, b) Pt(II)/NiF(H) and (c, d) SEM images of Pt(II)/NiF after the durability test.

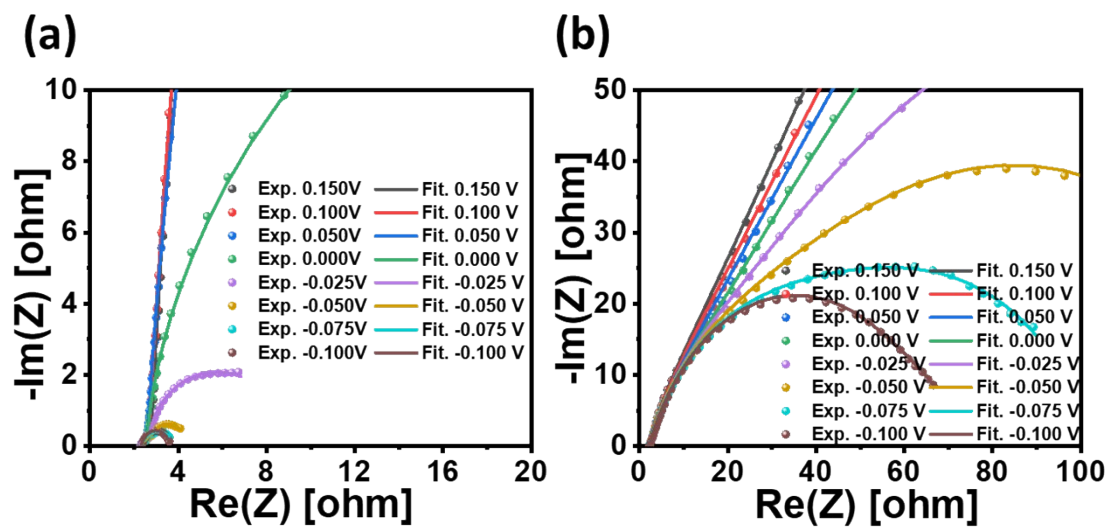


**Figure S9.** Experimental (Exp.) and fitting (Fit.) Nyquist plots for (a)Pt(II)/NiF(H) and (b) Pt(II)/NiF at different potentials.

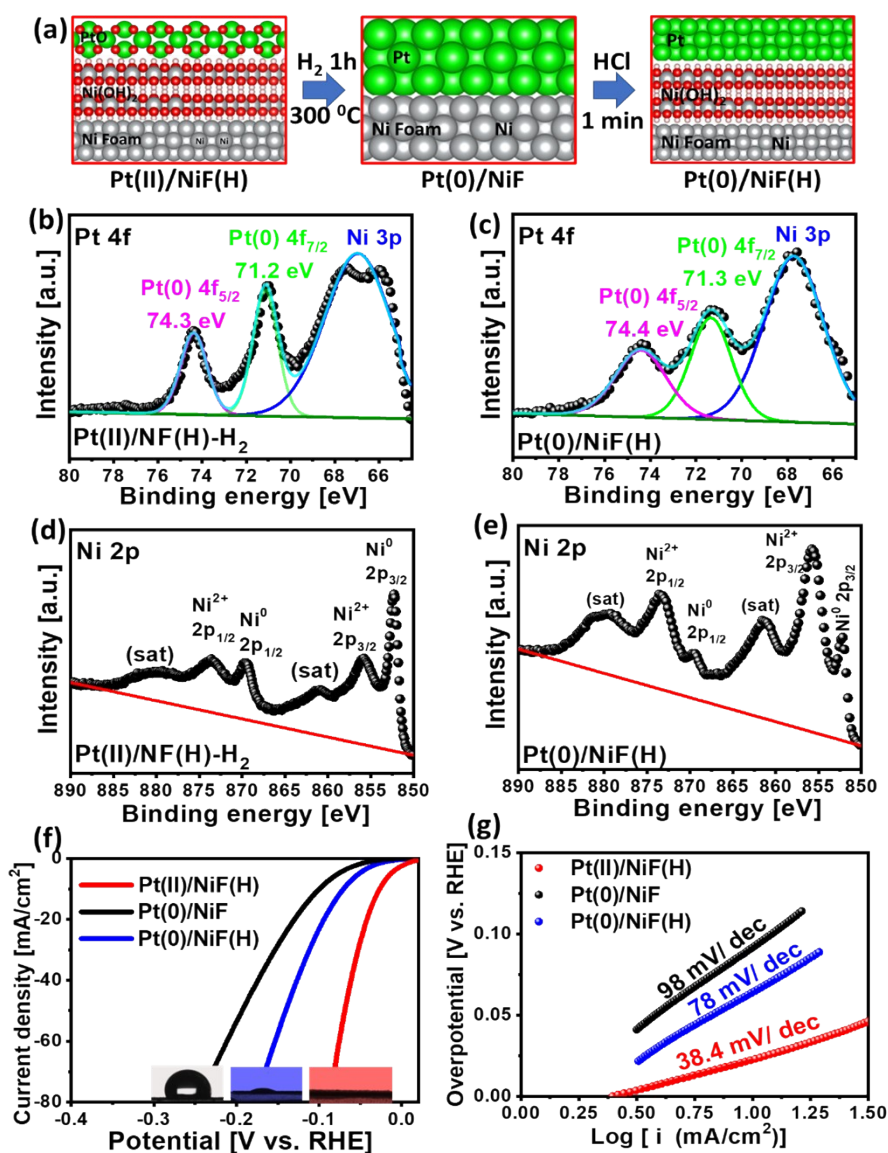


**Figure S10.** (a) Schematic illustration showing the preparation of Pt(0)/NiF, and Pt(0)/NiF(H). Pt 4f XPS spectra of (b) Pt(0)/NiF, and (c) Pt(0)/NiF(H). Ni 2p XPS spectra of (d) Pt(0)/NiF, and (e) Pt(0)/NiF(H). (f) LSV curves and (g) Tafel slopes for Pt(II)/NiF(H), Pt(0)/NiF, and Pt(0)/NiF(H).

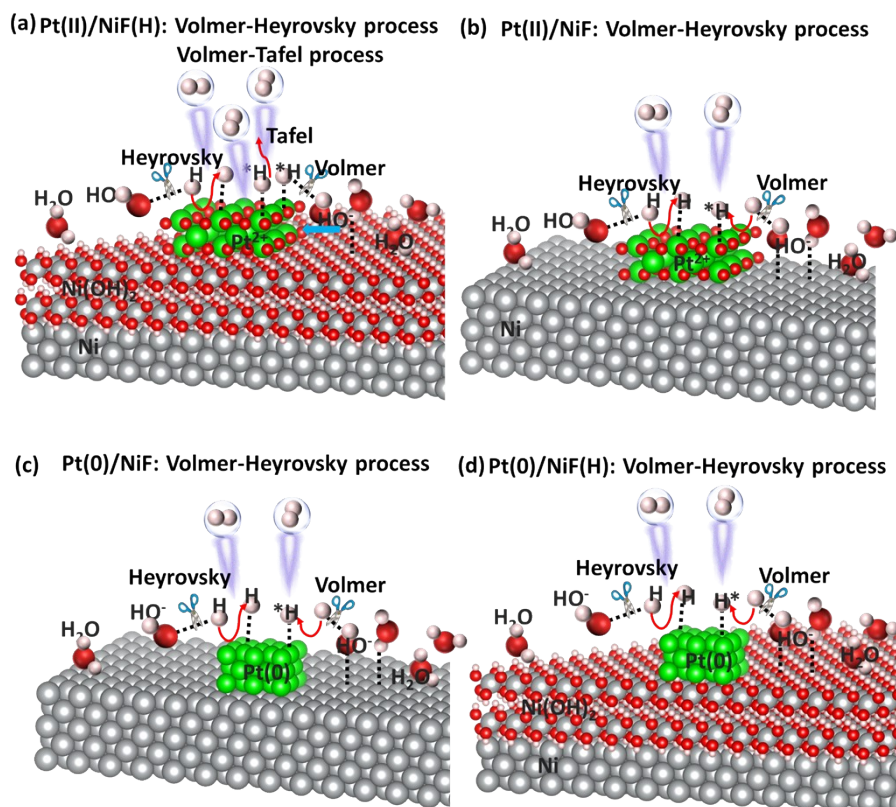


**Figure S11.** Illustrations of HER process on (a) Pt(II)/NiF(H), (b) Pt(II)/NiF, (c) Pt(0)/NiF, and (d) Pt(0)/NiF(H)

## References

- [1] G. Kresse, J. Hafner, Ab Initio molecular Dynamics for Liquid Metals, *Phys. Rev. B* 47 (1993) 558-561.
- [2] G. Kresse, J. Hafner, Ab initio molecular-dynamics simulation of the liquid-metalamorphous-semiconductor transition in germanium, *Phys. Rev. B Condens. Matter Mater. Phys.* 49 (1994) 14251–14269.
- [3] J. P. Perdew, K. Burke, M. Ernzerhof, Generalized Gradient Approximation Made Simple. *Phys. Rev. Lett.* 77 (1996) 3865-3868.
- [4] G. Kresse, D. Joubert, From ultrasoft pseudopotentials to the projector augmentedwave method, *Phys. Rev. B Condens. Matter Mater. Phys.* 59 (1999) 1758–1775.
- [5] S. Grimme, J. Antony, S. Ehrlich, H.A. Krieg, Consistent and accurate ab initio parametrization of density functional dispersion correction (DFT-D) for the 94 elements H-Pu, *J. Chem. Phys.* 132 (2010), 154104.
- [6] K. Momma and F. Izumi, *J. Appl. Crystallogr.*, 44, 1272-1276 (2011).